Fracture 1977, Volume 3, ICF4, Waterloo, Canada, June 19 - 24, 1977

AN EXPERIMENTAL AND FEM STUDY ON CRACK OPENING DISPLACEMENT

Albert S. Kuo and H. W. Liu*

INTRODUCTION

Wells [1] proposed crack tip opening displacement, δ_t, as a ductile fracture criterion at and beyond general yielding, and he verified the criterion experimentally with mild steel specimens. Recently, Green and Knott [2] have shown that δ_t, at the initiation of fibrous fracture, is a constant. McClintock [3] also proposed that fatigue crack growth per cycle is equal to half of the crack tip opening displacement. Ke and Liu [4] proposed near tip strain as a fracture criterion for ductile and tough materials, and they found a linear relationship between near tip strain and near tip crack opening displacement, δ. δ_t is related to the stress intensity factor K, in the case of small scale yielding, according to the strip yielding model [5 - 9]. Subsequently, it has been shown that δ is related to crack tip stresses and strains [10, 11]. All of these studies are two dimensional analyses which do not take into account the thickness consideration. In this study, the effect of thickness on crack opening displacement is studied experimentally. The results are further analyzed with the aid of the two-dimensional FEM calculations.

EXPERIMENTS AND RESULTS

Aluminum alloys, Al 2024-0, Al 2024-T3, and Al 2024-T351, were used in this study. The tensile yield strengths of these alloys were 53.8, 310, and 386 MPa, respectively. The specimens were 10.16 cm wide, with central cracks or central slots, $2a \simeq 1.78$ cm. All the specimens were centrally slotted, with the exception of specimens 4 and 5 which were centrally slotted with a jeweler's saw and then fatigue pre-cracked. The width of the slots was approximately 0.023 cm. Specimens of two different thicknesses, namely 0.041 cm and 0.625 cm, were tested.

Crack opening displacements, δ, between the upper and lower crack surfaces under static tensile load were measured with the moire method. The specimen surface was polished, cleaned, dried, and coated with photo-resist. A moire grille, of line density 5275 lines/cm, was printed onto the specimen surface with its grille lines perpendicular to the loading direction. The moire pattern was obtained by double exposures before and after deformation. A more detailed description of moire method was given by Schaefer, Liu and Ke [12]. The applied load and plate thickness were chosen to give a large plastic zone relative to plate thickness ($[K/\sigma_Y]^2/t \simeq 18$), and a small plastic zone relative to plate thickness ($[K/\sigma_Y]^2/t \simeq 1.12$).

The measured crack opening displacements will be compared with those calculated using the Dugdale model, the elastic model, and the elastic-plastic model. The crack opening displacements of an elastic crack in an infinite plate is given by Ang and Williams [13] as:

* Syracuse University, Syracuse, New York, 13210, U. S. A.

$$\delta = 4\,\sigma\,(a^2-x^2)^{1/2}/E \qquad \text{plane stress}$$
$$\delta = 4\,\sigma\,(1-\nu^2)\,(a^2-x^2)^{1/2}/E \qquad \text{plane strain,} \tag{1}$$

where 2a is the length of the crack laying along the x-axis with its tips at $x = \pm a$. ν, σ, and E are the Poisson's ratio, applied tensile stress, and Young's modulus, respectively. Goodier and Field [6] used the Dugdale model to calculate crack opening displacement, δ. For plane stress case,

$$\delta = \frac{2\sigma_Y\,(a+\ell)}{\pi E}\left[\cos\theta\,\ln\frac{\sin^2(\theta_2-\theta)}{\sin^2(\theta_2+\theta)} + \cos\theta_2\,\ln\frac{(\sin\theta_2+\sin\theta)^2}{(\sin\theta_2-\sin\theta)^2}\right. \tag{2}$$

where σ_Y is the tensile yield strength, ℓ is the length of the strip yielding zone and $\ell = a(\sec\theta_2-1)$, $\theta_2 = \pi\sigma/2\,\sigma_Y$, $\cos\theta = x/(a+\ell)$ for $|x| < (a+\ell)$, and $-\pi < \theta < \pi$. Similar results, using the continuous dislocation model, were obtained by Bilby, Cottrell, and Swinden [9].

Specimens 1 and 2 were made of the aluminum alloy, Al 2024-0, and both were loaded to the same K-value, 4.53 MPa$\cdot$m$^{1/2}$. Both specimens were slotted, but were of different thicknesses: 0.041 cm and 0.625 cm, respectively. The values of the quantity, $(K/\sigma_Y)^2/t$, were 17.5 and 1.12 for these two specimens, where t was specimen thickness. The results of the measurements are shown in Figure 1.

In Figures 1, 2, and 3, the solid lines indicate the elastic calculation, equation (1), and the dashed lines indicate the Dugdale calculation, equation (2). The dash-dotted line in Figure 1b indicates the elastic-plastic FEM calculation, which agrees well with the elastic calculation in the region $r > 7.6 \times 10^{-2}$ cm. Figure 1 indicates that the measurements of specimen 1 agreed with the plane stress Dugdale calculation, but the measurements of specimen 2 agreed with the plane strain elastic calculation. It should be noted that, in the region of measurements, the results of the FEM elastic-plastic calculation coincided with those of the elastic calculation. Unfortunately, no measurements were made in the region closer to the crack tip.

Specimens 3 and 4 were made of Al 2024-T3, and their thicknesses: 0.041 cm and 0.038 cm were nearly the same. Specimen 3 was slotted, and specimen 4 was fatigue pre-cracked. The applied K-values of these two specimens 26.2 and 28.2 MPa$\cdot$m$^{1/2}$. The values of $(K/\sigma_Y)^2/t$ for these two specimens were 17.5 and 18.8 respectively. The results in Figure 2 show that the measurements of both specimens agreed well with the plane stress Dugdale calculation in spite of the slot in specimen 3.

Specimens 5 and 6 were made of Al 2024-T351 and were of same thickness, 0.625 cm. Specimen 5 was fatigue pre-cracked, and specimen 6 was slotted. These two specimens were loaded to the nearly same K-values, 20.4 and 20.9 MPa$\cdot$m$^{1/2}$. The values of $(K/\sigma_Y)^2/t$ for these two specimens were 0.45 and 0.46, respectively. The results in Figure 3 show that the cracked specimen agreed well with the plane strain elastic calculation, but the slotted specimen fell in between the Dugdale and the elastic calculations. At the applied load level, the Dugdale and the elastic crack opening displacements were very close of each other. A thicker specimen loaded to a higher stress level was needed to make a distinction between these two models.

In an earlier work [12], crack opening displacements were measured in a very thin steel specimen, $(K/\sigma_Y)^2/t = 48$. In the thin specimen, extensive crack tip deformation caused localized crack tip strip necking. The strip necking zone was embedded in a diffused plastic zone which, in turn was embedded in the massive elastic plate as shown schematically in Figure 4. The crack opening displacement measurements in the steel specimen agreed well with the Dugdale calculation as shown in Figure 5. Even the opening displacements in the strip yielding zone agreed reasonably well with the Dugdale calculation.

Figure 6 is a picture of the typical moire patterns near a crack tip. It was taken from specimen 4 which was only 0.038 cm thick, and was loaded to K = 28.2 MPa$\cdot$m$^{1/2}$. The heavily deformed plastic region appeared to be diffused. However, there was a slight indication in the picture that the plastic zone had the tendency to become strip-necked. The measurements of specimen 4 agreed with the Dugdale model as was mentioned earlier, even without a strip necking zone.

CALCULATION OF δ WITH THE FEM

Crack opening displacements were calculated with the finite element method under the conditions of plane strain and small scale yielding. In a region, r_e, near a crack tip, the elastic stresses are [15, 16]:

$$\sigma_{ij} = [K/(2\,\pi\,r)^{0.5}]f_{ij}(\theta) \tag{3}$$

where r and θ are the polar coordinates with the origin at the crack tip. The crack line lies along the negative x-axis. K is the mode I stress intensity factor. In the case of small scale yielding, a small plastic zone, r_p, is embedded in the elastic crack tip stress field. If $r_p \ll r_e$, according to Saint Venant's principle, it could be shown that a relaxation of the stresses in the plastic zone would not significantly change the stresses on the boundary of r_e. Therefore, for the case of small scale yielding, the crack tip deformation could be obtained from the calculation on a semi-circular region with the boundary stresses given by equation (3), [17].

The configuration of the elements is shown in Figure 7. There are 372 elements and 213 nodes. The smallest element at the crack tip is 5.33×10^{-3} cm with a crack length of 2.54 cm. Plane-strain and constant-strain elements are used. The computer programme is based on the elastic-plastic constitutive matrix obtained by Yamada and Yoshimura [18]. The values of yield strength, Young's modulus, strain-hardening exponent, and Poisson's ratio are 53.8 Pa, 68.9×10^3 Pa, 0.307, and 0.3, respectively.

The calculated crack opening displacements are shown in Figure 8. The different symbols in the figure denote the calculated values at different K-values. Close to the crack tip, δ could be expressed as,

$$\delta/r_p = \beta\,(r/r_p)^m \quad , \quad \beta = (\delta/r_p)_{r=r_p} \, . \tag{4}$$

The value of the slope, m, is 0.37. The value of m from HRR singularity analysis [10, 11] is 0.23. β is the value of δ/r_p at $r = r_p$; its value is 3.5×10^{-3} found from Figure 8. r_p is the plastic zone size, along the

$\theta = 60°$ line, and it is related to K,

$$r_p = \alpha\ (K/\sigma_Y)^2 = 0.112\ (K/\sigma_Y)^2 \ . \qquad (5)$$

The value of α, 0.157, was obtained by Levy et al [17] using the FEM for a non-hardening material, along the line $\theta = 70°$, where r_p is maximum.

Combining equation (4) and equation (5), one has the following relation for δ

$$\delta = \beta\ \alpha^{1-m}(K/\sigma_Y)^{2(1-m)} r^m = 8.74 \times 10^{-4}(K/\sigma_Y)^{1.27} r^{0.37} \ . \qquad (6)$$

A comparison of the δ calculated by using the Dugdale model, the elastic model, and the elastic-plastic model by the FEM is shown in Figure 9. It is evident from the figure that near the crack tip, the Dugdale model gives a much higher value of δ than either the elastic model or the elastic-plastic model.

In the region $r/(K/\sigma_Y)^2 < 0.13$, the values given by FEM elastic-plastic calculation and the elastic results diverge as r approaches the crack tip. In the region $r/(K/\sigma_Y)^2 > 0.13$, the elastic-plastic calculation coincides with the elastic solution. This is also shown in Figure 1b. The moire measurements fell into the range where the FEM calculations and the elastic results coincide. In order to see the difference between the elastic and the elastic-plastic models, the measurements would have to be made in the region closer to the crack tip.

The Dugdale model is based on the physical model of strip yielding. In the experimental moire study, no strip yielding has been observed. The quantity $(K/\sigma_Y)^2/t$ is a measure of the size of plastic zone relative to thickness, and it is also an index of the deviation from the plane strain condition. When a specimen is very thin, for example, for the thin steel specimen at $(K/\sigma_Y)^2/t = 48$, strip necking takes place. The strip necking zone is embedded in a diffused plastic zone. In this case, the Dugdale calculation agrees well with the measurements. As the specimen thickness is increased, the strip necking zone disappears. However, the Dugdale model for the calculation of δ is still applicable in the region $(K/\sigma_Y)^2/t > 18$, even without a strip necking zone. As the plate thickness is further increased, and the applied K-value is reduced to the point $(K/\sigma_Y)^2/t < 1$, the Dugdale model δ differs considerably from the moire measurement. In this region, the measurements agree well with the elastic solution. In the region of measurements, the elastic solution coincides with the elastic-plastic FEM calculation. It is expected that in the region closer to a crack tip, the measurements would agree with the elastic-plastic calculation.

CRACK TIP OPENING DISPLACEMENT, δ_t, AND THE UNZIPPING MODEL

Based on the empirical results shown earlier, it is expected that δ_t calculated with the Dugdale model, is an appropriate measure of crack tip deformation only for thin specimens loaded to high K-values. The calculated δ_t with the Dugdale model by Goodier and Field [6] is

$$\delta_t = (8\ \sigma_Y\ a/\pi E)\ \ln\ [\sec(\pi\sigma/2\ \sigma_Y)] \ . \qquad (7)$$

Based on the Dugdale model, in the case of small scale yielding, Rice obtained [7],

$$\delta_t = K^2/E\ \sigma_Y \ . \qquad (8)$$

Subsequently, δ_t was calculated by Levy et al using the FEM [17],

$$\delta_t = 0.425\ K^2/E\ \sigma_Y \ . \qquad (9)$$

δ_t given by these models could be used to characterize crack tip deformations and stresses in the analyses of brittle and ductile fractures.

McClintock and Pelloux [3, 19] suggested that fatigue crack growth rate, da/dN, is related to δ_t, for the decohesion plane inclined 45° to the crack plane. Recently, Kuo and Liu [21] made a calculation of the crack tip opening displacement and the crack tip advancing based on the unzipping model of shear decohesion taking place on two conjugate decohesion planes as shown schematically in Figure 10. As the applied stress on a cracked solid is increases, the decohesion processes take place along slip lines, α, b, β, c, γ, and d successively; while the "slabs' between the neighbouring slip lines move like the teeth of a zipper during the unzipping process, causing crack tip opening and advancing. The unzipping model separates the crack tip opening which contributes to crack tip advancing from those which cause crack tip blunting. Crack growth rate is related to δ_t, which in turn is related to ΔK. The final result is

$$da/dN = 0.019\ (1-\nu^2)\ K^2/E\ \sigma_{Y(c)} \qquad (10)$$

where $\sigma_{Y(c)}$ is the cyclic yield strength. If the ratio of the cyclic yield strength to the Young's modulus is 1/400, the agreement between the predicted crack growth rates and the empirical rates given by Barsom [22], Hahn et al [23] and Bates and Clark [24], is within a factor of 2; while the calculated growth rates, according to the classic Dugdale model, are more than 10 times higher than the empirical rates.

It can be concluded that the Dugdale model is applicable for analyzing δ and δ_t only in thin specimens loaded to high K-values. For a thick specimen at a low K-value, the general contour to the crack tip is, perhaps, better described by the elastic-plastic FEM calculations, such as those given by Levy et al. The crack tip opening which contributed to crack tip advancing is more realistically given by the unzipping model.

ACKNOWLEDGEMENTS

The authors wich to thank NSF (Grant No. GK-34047) for their support and Mrs. H. Turner and Mr. R. Ziemer for the preparation of the manuscript.

REFERENCES

1. WELLS, A. A., British Welding J., Nov., 1963, 563.
2. GREEN, G. and KNOTT, J. F., J. Eng. Mat. and Tech., Jan., 1976, 37.
3. McCLINTOCK, F. A., Fatigue Crack Propagation, ASTM STP 415, 1967, 170.
4. KE, J. S. and LIU, H. W., Int. J. of Fracture, 7, 1971, 487.
5. DUGDALE, D. S., J. of Mech. and Phys. of Solids, 8, 1960, 100.

6. GOODIER, J. N. and FIELD, F. A., Fracture of Solids, John Wiley, New York, 1963, 103.
7. RICE, J. R., Fatigue Crack Propagation, ASTM STP 415, 1967, 247.
8. RICE, J. R., J. of Appl. Mech., June, 1968, 379.
9. BILBY, B. A., COTTRELL, A. H. and SWINDEN, K. H., Proc. Roy. Soc., London, A285, 1965, 304.
10. HUTCHINSON, J. W., J. of Mech. and Phys. of Solids, 16, 1968, 13.
11. RICE, J. R. and ROSENGREN, G. F., J. of Mech. and Phys. of Solids, 16, 1968, 1.
12. SCHAEFFER, B. J., LIU, H. W. and KE, J. S., Exp. Mechanics, April, 1971, 172.
13. ANG, D. D. and WILLIAMS, M. L., J. of Appl. Mech., Sept., 1961, 372.
14. McCLINTOCK, F. A., ASME, J. of Basic Eng., 82, 1960, 423.
15. WILLIAMS, M. L., J. of Appl. Mech., March, 1957, 109.
16. IRWIN, G. R., J. of Appl. Mech., Sept., 1957, 361.
17. LEVY, N., MARCAL, P. V., OSTERGREN, W. J. and RICE, J. R., Int. J. of Fracture Mech., 7, 1971, 143.
18. YAMADA, Y. and YOSHIMURA, N., Int. J. of Mech. Sci., 10, 1968, 343.
19. PELLOUX, R. M. N., Trans. ASM, 62, 1969, 281.
20. HU, W. L. and LIU, H. W., Proceedings of ICM-II, published by ASM, 1976, 1058.
21. KUO, A. S. and LIU, H. W., Scripta Metallurgica, 10, 1976, August, 723.
22. BARSON, J. M., Damage Tolerance in Aircraft Structures, ASTM STP 486, 1971, 1.
23. HAHN, G. T., HOAGLAND, R. C. and ROSENFIELD, A. R., AF 33615-70-C-1630, Battelle Memorial Inst., Columbus, Ohio, August, 1971.
24. BATES, R. C. and CLARK, W. G., Jr., Trans. ASM., 62, 1969, 380.

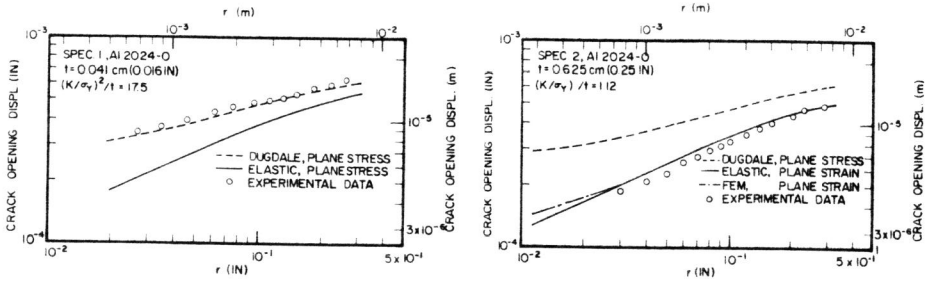

(a) (b)

Figure 1 Effect of Thickness on δ, Al 2024-0 Aluminum Alloy

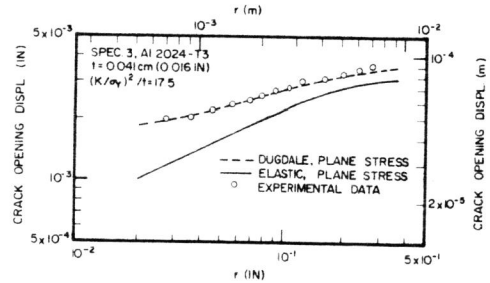

(a)

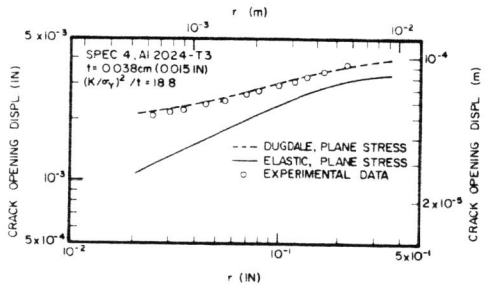

(b)

Figure 2 δ in Al 2024-T3 Aluminum Alloy

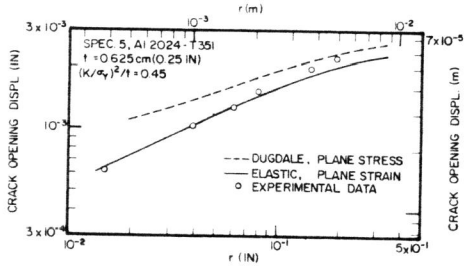

(a)

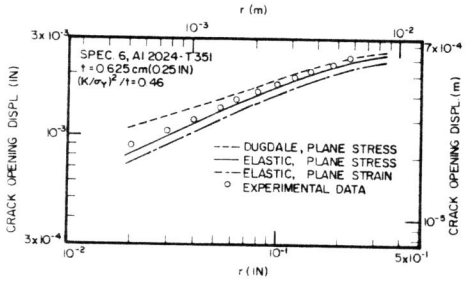

(b)

Figure 3 δ in Al 2024-T351 Aluminum Alloy

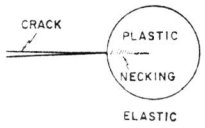

Figure 4 Schematic Diagram of Crack Tip Necking [14]

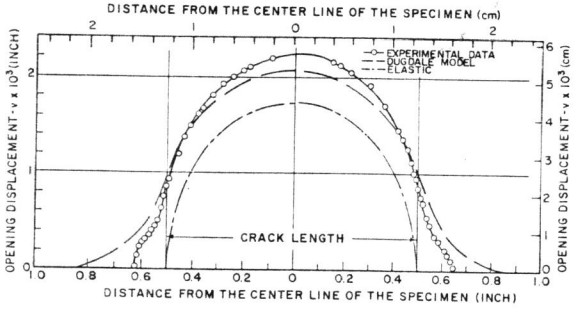

Figure 5 δ in Thin Steel Specimen [12]

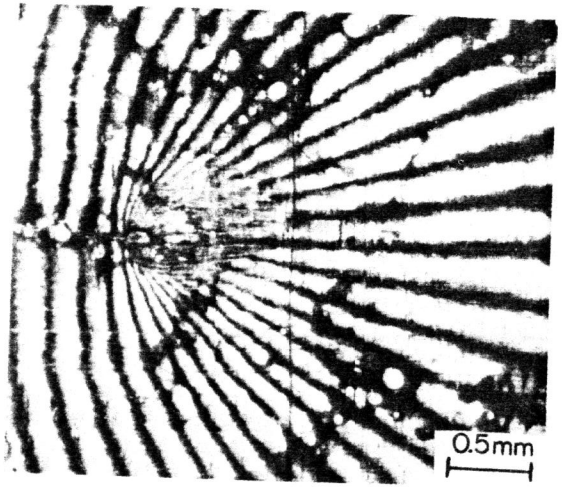

Figure 6 Moire Pattern at Crack Tip

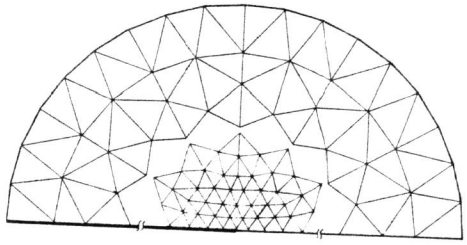

Figure 7 FEM Element Configuration

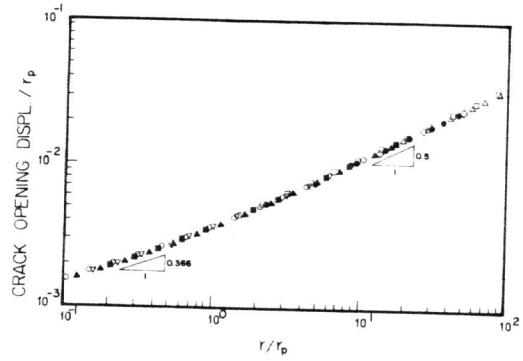

Figure 8 δ by Elastic-Plastic FEM Calculation - Small Scale Yielding

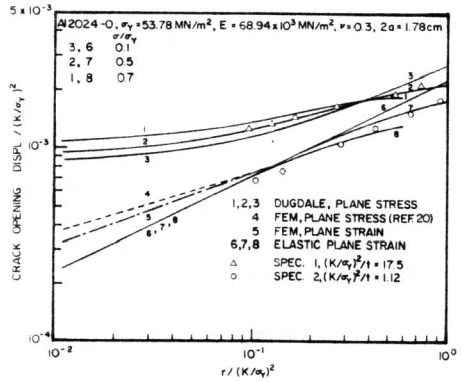

Figure 9 δ - A Comparison of Dugdale, Elastic and Elastic-Plastic Models

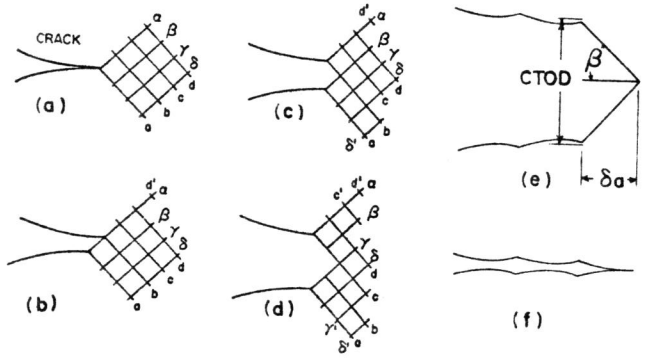

Figure 10 Unzipping Model for Crack Tip Opening and Advancing [21]